High pressure Raman investigations of multiferroic $BiFeO_3$

2009 J. Phys.: Condens. Matter 21 385901

(http://iopscience.iop.org/0953-8984/21/38/385901)

J. Phys.: Condens. Matter **21** (2009) 385901 (5pp) doi:10.1088/0953-8984/21/38/385901

High pressure Raman investigations of multiferroic $BiFeO_3$

Y Yang[1], L G Bai[2], K Zhu[1], Y L Liu[1,4], S Jiang[2], J Liu[2], J Chen[3] and X R Xing[3]

[1] Institute of Physics, Chinese Academy of Sciences, Beijing 100190, People's Republic of China
[2] Institute of High Energy Physics, Chinese Academy of Sciences, Beijing 100049, People's Republic of China
[3] Department of Physical Chemistry, University of Science and Technology Beijing, Beijing 100083, People's Republic of China

E-mail: ylliu@aphy.iphy.ac.cn

Received 27 February 2009, in final form 6 July 2009
Published 24 August 2009
Online at stacks.iop.org/JPhysCM/21/385901

Abstract

We have reported a Raman scattering investigation of bismuth ferrite ($BiFeO_3$) under high pressure up to 50 GPa. Distinct changes in the Raman spectra show evidence for three pressure-induced structural transitions. The abrupt frequency redshifts of the Raman modes near 300 cm^{-1} at around 3 GPa are attributed to the modulation of the FeO_6 octahedral tilts. The disappearance of the modes below 250 cm^{-1} at 8.6 GPa, together with the enhancement of the two modes in the range of 300–400 cm^{-1}, indicate the phase transition from the rhombohedral to orthorhombic symmetry. Afterward, the E-3 and E-4 modes disappear at 44.6 GPa, pointing to the occurrence of the orthorhombic–cubic phase transition, which is consistent with the previous postulate that an orthorhombic–cubic transition takes place across the metal–insulator transition at high pressures.

1. Introduction

Magnetoelectric (ME) multiferroics have attracted a great deal of attention in recent years because of their basic physical properties and potential applications in data storage, spintronics and quantum electromagnets [1–4]. $BiFeO_3$ is one of the most intensively studied multiferroic materials since it exhibits simultaneously antiferromagnetic and ferroelectric properties at room temperature [5]. Many theoretical and experimental research works, such as x-ray diffraction (XRD), scanning electronic microscopy (SEM) and Raman spectroscopy, have been performed in order to characterize the properties of $BiFeO_3$ as well as its structure [6–15]. Although the structure of $BiFeO_3$ has been extensively studied by various methods, its structural behavior under external conditions, such as high temperature and high pressure, remains controversial [4]. High pressure investigations would provide important pressure instabilities on the local and average scale, which is in contrast to the effect of temperature that only lead to an average evolution of crystal structure. Through first-principles calculations, Rabindran *et al* predicted that a pressure-induced phase transition from the rhombohedral ($R3c$) phase to orthorhombic ($Pnma$) symmetry occurs at around 13 GPa [8]. In a recent report, Palai *et al* observed an insulator–metal transition together with an orthorhombic–cubic phase transition in $BiFeO_3$ in the temperature range of 1203–1230 K [14]. According to the high temperature experiments, they postulated that the same transition sequence would be observed in a diamond anvil cell experiment at about 47 GPa. In addition, Gavriliuk *et al* observed indirectly an insulator–metal transition in $BiFeO_3$ at a high pressure of ~47 GPa [11]. However, the structural phase of $BiFeO_3$ at high pressures is still unclear. Therefore, it is crucial to carry out further investigations into the structure and other physical properties of $BiFeO_3$ under high pressures.

Micro-Raman spectroscopy has been proved to be a convenient method to study the phase transition and local structure modulation in ferroelectric materials [12–14, 16–19]. In principle, any changes in the crystal structure or physical properties can be revealed in frequency, bandwidth and intensity of the Raman peaks. Although the lattice dynamics in $BiFeO_3$ have been intensively investigated, limited literature

[4] Author to whom any correspondence should be addressed.

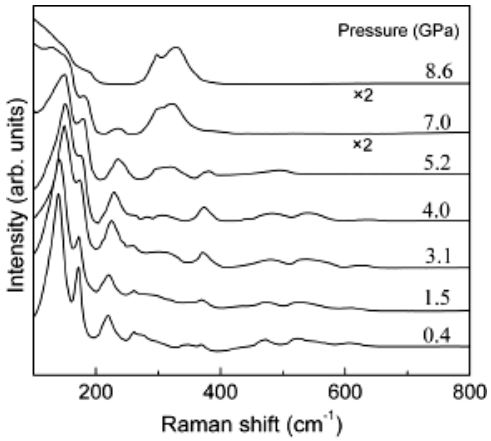

Figure 1. Representative Raman spectra of $BiFeO_3$ measured in the pressure range of 0–8.6 GPa.

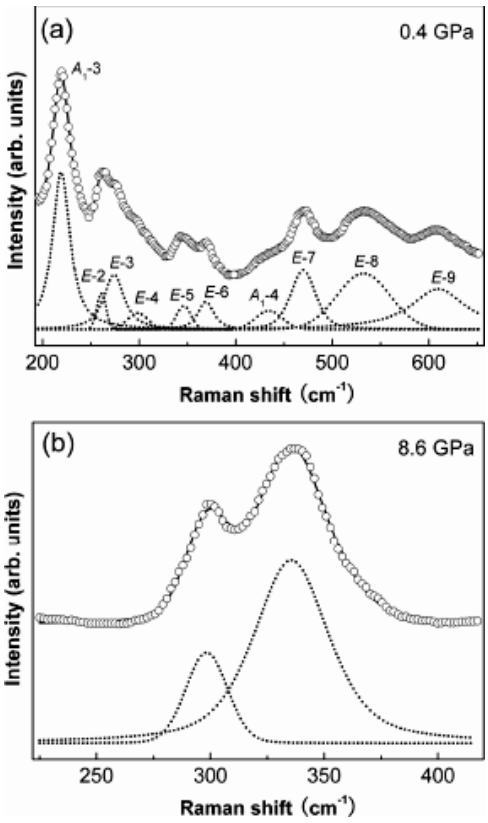

Figure 2. Representative Lorentzian-shape deconvolutions of the mid-frequency Raman spectra measured at two selected pressures.

about the high pressure Raman investigations of $BiFeO_3$ has been reported [12]. Furthermore, Raman spectroscopy for $BiFeO_3$ under high pressures up to 50 GPa has not been presented. In this paper, we reported a systematic Raman study of the effects of high pressure on the structure of $BiFeO_3$. Prominent changes in the Raman spectra indicate the occurrence of three structural transitions in $BiFeO_3$. These results provide further information for understanding the coupling between the structure and other properties of $BiFeO_3$ under high pressures.

2. Experimental details

$BiFeO_3$ powder with a single-phase rhombohedral $R3c$ structure is prepared by a molten salt synthesis (MSS) method which was recently reported in detail in another publication [20]. High pressure Raman experiments were performed at room temperature using a modified Mao–Bell diamond anvil cell. The culet size of the diamond anvil was 300 μm in diameter. A 300 μm thick steel gasket (T301) was preindented to 30 μm thickness (120 μm initial hole diameter). The 4:1 methanol–ethanol mixture was used as a pressure-transmitting medium. The pressure was calibrated using the ruby fluorescence method. Raman spectra were measured in the backscattering geometry using a confocal micro-Raman spectrometer (Jobin Yvon HR800) with the 532 nm laser line as excitation source. A 25× microscope objective was used in order to focus the laser beam and collect the scattered light. All the measurements were carried out at room temperature.

3. Results and discussions

Figure 1 presents the Raman spectra of $BiFeO_3$ collected in the pressure range of 0–8.6 GPa. Looking at the bottom line presented in figure 1, the spectrum measured at ambient condition exhibits good agreement with that reported previously [13, 14]. According to the group theory, 13 Raman-active modes are predicted for $BiFeO_3$ with rhombohedral structure ($R3c$): $\Gamma_{\text{Raman}} = 4A_1 + 9E$. Except for the A_1 mode below 100 cm^{-1}, which cannot be observed due to the rejection of the notch filter in the spectrometer, all the other Raman modes are observed in the spectra. Three sharp peaks at around 139, 170 and 220 cm^{-1} are assigned as A_1 modes. Nine weak peaks are located in the range of 250–650 cm^{-1}, which are clearly discernible in figure 2(a). Besides the A_1 mode at 433 cm^{-1}, the other modes are in the E-symmetry. As presented in figure 1, the Raman peaks below 250 cm^{-1} shift to higher frequency and broaden gradually with increasing pressure. This phenomenon is due to the pressure-induced bond shortening and lattice distortion. It is striking to find that the peak at around 370 cm^{-1} (denoted as E-6 mode) increases at first, then begins to decrease at 3 GPa and disappears at 7.01 GPa. Such an anomaly may be correlated with a structural reordering in $BiFeO_3$, at least locally. On the other hand, the E-3 and E-4 modes at 274 and 298 cm^{-1}, respectively, show prominent successive enhancement. When pressure is up to 8.6 GPa, these two peaks can be seen apparently at 295 and 327 cm^{-1}, whereas the other Raman peaks disappear. In order to investigate the further pressure evolution of these two peaks, Raman spectra were measured in the high pressure range (8.6–50 GPa) and displayed in figure 3. The E-3 and E-4 modes shift progressively to higher frequency range with further increasing pressure. It is noteworthy that E-3 declines faster than E-4 and disappears at around 38.7 GPa, while peak E-4 remains until 44.6 GPa.

The frequency positions of all the observed Raman modes are plotted as a function of pressure in figure 4, in which two prominent spectral features can be seen clearly. Firstly, it can

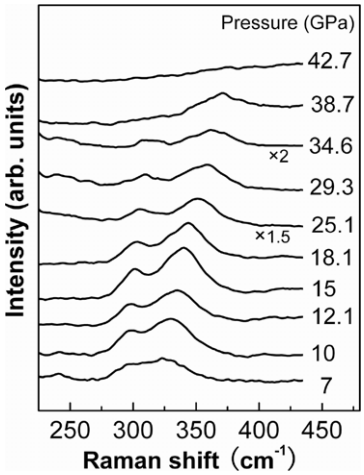

Figure 3. Representative Raman spectra of $BiFeO_3$ measured in the pressure range of 7–44.6 GPa.

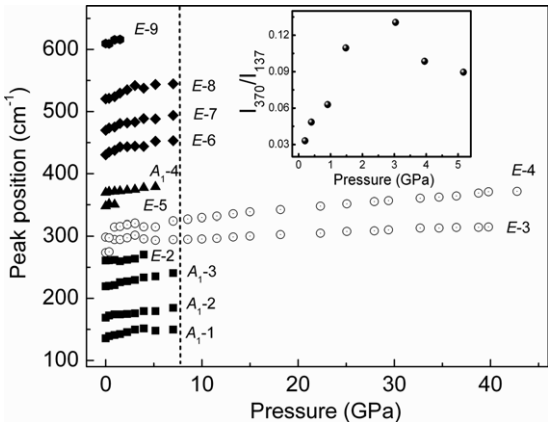

Figure 4. Pressure-dependent evolution of the peak position of selected Raman modes. The vertical dotted lines indicated the pressures at which the transitions take place. The inset shows the intensity ratio of the E-6 mode to the A_1-1 mode in the pressure range of 0–6 GPa.

be seen that, except for the E-3 and E-4 modes, all the other modes shift linearly to the higher frequency with increasing pressure and disappear at 8.6 GPa. Another prominent feature displayed in figure 4 is the abnormal behavior of the Raman peaks E-3 and E-4 in the low pressure range (0.1–6 GPa). The frequencies of E-3 and E-4 rise sharply at a rate of ∼4 cm^{-1} GPa^{-1} in the pressure range of 0.1–3 GPa, then decrease by ∼3 cm^{-1} GPa^{-1} between 3 and 5 GPa, and increase linearly with rates of 0.62 cm^{-1} GPa^{-1} and 1.32 cm^{-1} GPa^{-1}, respectively, with further increasing pressure. Such a phenomenon is similar to the intensity evolution of the E-6 mode near 370 cm^{-1}, which is shown in figure 1. As presented in the inset of figure 4, the intensity ratio of the E-6 mode to the A_1-1 mode at around 136 cm^{-1} reaches its maximum value at 3 GPa, beyond which it decreases quickly.

Thus, from the variations of Raman spectra exhibited in figures 1–4, we infer that $BiFeO_3$ undergoes three structural transitions under high pressures. The first structural rearrangement takes place at around 3 GPa, shown by the anomaly of the E-3 and E-4 modes. Analogous to the typical ferroelectric $BaTiO_3$, the Raman modes for $BiFeO_3$ over 200 cm^{-1} are attributed to the stretching and bending modes of the FeO_6 octahedra [15]. The pressure-induced negative frequency shift of the octahedra vibration modes for the typical ferroelectrics, such as $BaTiO_3$ and $PbTiO_3$, has been attributed to the change in the cation–anion displacement [16] and the appearance of the octahedral tilts [17]. The similar frequency anomaly was also observed in the rhombohedral $Na_{0.5}Bi_{0.5}TiO_3$ and ascribed to the displacement of the Ti^{3+} ion and the changes in the tilt system [18]. Therefore, the frequency anomalies of E-3 and E-4 modes of $BiFeO_3$ near 3 GPa can be interpreted by the changes in the displacement of B-site cations and the octahedral tilts. In the case of $BiFeO_3$, which is a highly distorted perovskite with rhombohedral structure, the cations and anions are displaced to one another along the [111] axis. Under applied high pressure, the volume of the unit cell is compressed, consequently leading to the reduction of the octahedral tiling.

Besides the structural modulation near 3 GPa, $BiFeO_3$ undergoes two further prominent phase transitions, as illustrated in figure 3. The first phase transition takes place at the pressure of 8.6 GPa, shown by the disappearance of the modes below 250 cm^{-1}. According to the theoretical calculation result, a pressure-induced phase transition from the rhombohedral ($R3c$) symmetry to the orthorhombic ($Pnma$) symmetry in $BiFeO_3$ is expected to be observed at around 13 GPa [8]. Moreover, Pashkin *et al* observed the rhombohedral–orthorhombic transition in $BiFeO_3$ at 7.5 GPa through far-IR reflectivity measurement [15]. Therefore, the phase transition observed at 8.6 GPa in our work could be tentatively ascribed to the rhombohedral–orthorhombic phase transition. What is more, the spectra measured at the pressures upon 8.5 GPa show great similarity with the spectra for the orthorhombic phase observed in the high temperature Raman experiment [14]. The frequency discrepancy of the Raman modes between our results and that in [14] may be attributed to the difference between the temperature-induced redshift and pressure-induced blueshift. Four Raman-active modes are predicted for $BiFeO_3$ with orthorhombic structure since there is only one formula in one unit cell [14]. However, only two Raman modes are observed in our results. One possible explanation may be that these phonon peaks are too weak to be discernible and are covered by the intense background under higher pressures. Based on the previous literature, our results demonstrate the existence of the pressure-induced rhombohedral–orthorhombic phase transition in $BiFeO_3$. In addition, Kreisel *et al* pointed out that an intermediate phase arose from the changes in the octahedral system taking place across the rhombohedral–orthorhombic phase transition which makes such a transition more energetically plausible [18]. Therefore, according to the phase transition sequence observed in $BiFeO_3$, it is proved that a structure modulation has taken place at around 3 GPa.

The second phase transition is indicated by the disappearance of the E-3 and E-4 modes at 44.6 GPa, as presented in figures 3 and 4. Such spectral signatures directly

Table 1. The ambient-pressure phonon frequencies ω_{0i}, pressure derivatives of frequencies $\mathrm{d}\omega_i/\mathrm{d}p$ and mode Grüneisen parameters γ_i for various Raman modes of $BiFeO_3$ in low pressure and high pressure phases.

Low pressure (rhombohedral) phase				High pressure (orthorhombic) phase			
Raman mode	ω_{0i} (cm^{-1})	$\mathrm{d}\omega_i/\mathrm{d}p$ (cm^{-1} GPa^{-1})	γ_i	Raman mode	ω_{0i} (cm^{-1})	$\mathrm{d}\omega_i/\mathrm{d}p$ (cm^{-1} GPa^{-1})	γ_i
A_1-1	135.7	2	1.94				
A_1-2	168.9	2.24	1.74				
A_1-3	218	3.25	1.95				
E-2	260.9	0.47	0.23				
E-3	274.9	3.84	1.83	E-3	294.5	0.62	0.29
E-4	298.5	3.94	1.73	E-4	324.2	1.32	0.56
E-5	347.7	2.72	1.02				
A_1-4	369.5	1.78	0.63				
E-6	430.4	3.23	1.04				
E-7	469.8	3.42	0.95				
E-8	520.4	3.45	0.87				
E-9	609.5	4.28	0.92				

demonstrate the structural transition from the orthorhombic phase to cubic phase, since $BiFeO_3$ with cubic structure has no Raman-active modes. Gavriliuk *et al* have observed an abrupt change in the unit cell volume in the pressure range 40–50 GPa, which was accompanied by the insulator–metal transition, but gives no more detailed definition [11]. Based on the high temperature experiments, Scott and Palai *et al* postulated that an orthorhombic–cubic phase transition should accompany with an insulator–metal transition [4, 14]. The results in our experiment demonstrate directly that an orthorhombic–cubic phase transition would take place in $BiFeO_3$ during the insulator–metal transition at high pressures. Unlike the classical ferroelectric $PbTiO_3$ [17] and the relaxor ferroelectric $PbZn_{1/3}Nb_{2/3}O_3$ [19], which are still in the ferroelectric phase at the very high pressure region, $BiFeO_3$ transfers into the cubic structure at ∼47 GPa. This phenomenon could be associated with the magnetic and electronic properties of $BiFeO_3$. A magnetic transition from the magnetically ordered state to the nonmagnetic state was observed at around 47 GPa through Mössbauer spectroscopy [21]. Gavriliuk *et al* attributed the high-pressure-induced insulator–metal transition in $BiFeO_3$ to the spin crossover from the high spin (HS) state to the low spin (LS) state. It is generally believed that the interaction between structure, magnetic and electronic properties exists in $BiFeO_3$. The structure phase transition, magnetic collapse and insulator–metal transition taking place at the same pressure point (∼47 GPa) undoubtedly demonstrates the close relation of these order parameters. The disappearance of the ferroelectricity in $BiFeO_3$ due to the orthorhombic–cubic phase transition is naturally connected with the pressure-induced changes of the other two properties.

It is well known that the Grüneisen parameter γ plays a crucial role in understanding the thermodynamic and thermoelastic behavior of solids. The slopes of phonon frequency versus pressure curves are calculated according to the results displayed in figure 4 and listed in table 1, which are useful to calculate the mode Grüneisen parameters. Table 1 lists the ambient-pressure phonon frequencies ω_{0i}, their pressure derivatives $\mathrm{d}\omega_i/\mathrm{d}p$ and mode Grüneisen parameters γ_i for both phases of $BiFeO_3$. The mode Grüneisen parameters for the low and high pressure phases were calculated using the formula: $\gamma_i = (B_0/\omega_{0i})(\mathrm{d}\omega_i/\mathrm{d}p)$, where B_0 and ω_{0i} are the bulk modulus and the ambient-pressure phonon frequencies, respectively. Rabindran *et al* have put forward a theoretical result, in which the bulk modulus are $B_{01} = 130.9$ GPa for the rhombohedral phase and $B_{02} = 138.8$ GPa for the orthorhombic phase, respectively [8]. The $\mathrm{d}\omega_i/\mathrm{d}p$ and the orthorhombic phase ω_{0i} come from the linear fitting results as described in figure 3. According to the expression of Grüneisen parameters, γ_i is in direct proportion to the $\mathrm{d}\omega_i/\mathrm{d}p$, suggesting the bigger the pressure derivative of ω_i, the larger γ_i is. As given in table 1, in the lower pressure range, γ_{E-2} and γ_{A_1-4} is much smaller than the Grüneisen parameters for the other modes. This is consistent with the results presented in figure 4, in which the frequency blueshift rates for E-2 and A_1-4 modes are slower than those for the other modes. Moreover, the slope of $\mathrm{d}\omega_i/\mathrm{d}p$ for E-3 and E-4 in the higher pressure range is much smaller than that in the lower pressure range. The abrupt changes in the slopes of $\mathrm{d}\omega_i/\mathrm{d}p$ and Grüneisen parameters γ_i give the evidence of the rhombohedral–orthorhombic phase transition.

4. Conclusions

In summary, systematic Raman scattering was performed on $BiFeO_3$ in the pressure range of 0–50 GPa at ambient temperature. The evolution of the Raman spectra reveals that three structural transitions take place at around 3, 8.6 and 44.6 GPa, respectively. The first one is related with the pressure-induced distortion of the FeO_6 octahedra, while the second one is attributed to the rhombohedral–orthorhombic phase transition. These results show good agreement with the previous experimental and theoretical results. The last one is correlated with the orthorhombic–cubic phase transition, which supports directly the existence of the speculated pressure-induced insulator–metal transition. In addition, the mode Grüneisen parameters for the lower and higher pressure ranges were obtained.

Acknowledgments

This work was supported by the National Nature Science Foundation of China under grant nos. 10674171 and 10874236.

References

[1] Wang J, Neaton J B, Zheng H, Nagarajan V, Ogale S B, Liu B, Viehland D, Vaithyanathan V, Schlom D G, Waghmare U V, Spaldin N A, Rabe K M, Wuttig M and Ramesh R 2003 *Science* **299** 1719

[2] Eerenstein W, Mathur N D and Scott J F 2006 *Nature* **442** 759

[3] Ramesh R and Spaldin N A 2007 *Nat. Mater.* **6** 21

[4] Scott J F, Palai R, Kumar A, Singh M K, Murari N M, Karan N K and Katiyar R S 2008 *J. Am. Cream. Soc.* **91** 1762

[5] Fischer P, Połomska M, Sosnowska I and Szymański M 1980 *J. Phys. C: Solid State Phys.* **13** 1931

[6] Yun K Y, Noda M and Okuyama M 2003 *Appl. Phys. Lett.* **83** 3981

[7] Qi X, Dho J, Tomov R, Blamire M G and Driscoll J L M 2005 *Appl. Phys. Lett.* **86** 062903

[8] Ravindran P, Vidya R, Kjekshus A and Fjellvag H 2006 *Phys. Rev.* B **74** 224412

[9] Wang D H, Yan L, Ong C K and Du Y W 2006 *Appl. Phys. Lett.* **89** 182905

[10] Zavaliche F, Shafer P, Ramesh M R, Cruz P, Das R R, Kim D M and Eom C B 2005 *Appl. Phys. Lett.* **87** 252902

[11] Gavriliuk A G, Struzhkin V V, Lyubutin I S, Ovchinnikov S G, Hu M Y and Chow P 2008 *Phys. Rev.* B **77** 155112

[12] Haumont R, Kreisel J and Bouvier P 2006 *Phase Transit.* **79** 1043

[13] Ramirez M O, Krishnamurthi M, Denev S, Kumar A, Yang S, Chu Y, Saiz E, Seidel J, Pyatakov A P, Bush A, Viehland D, Orenstein J, Ramesh R and Gopalan V 2008 *Appl. Phys. Lett.* **92** 022511

[14] Palai R, Katiyar R S, Schmid H, Tissot P, Clark S J, Robertson J, Redfern S A T, Catalan G and Scott J F 2008 *Phys. Rev.* B **77** 014110

[15] Pashkin A, Rabia K, Frank S, Kuntscher C A, Haumont R, Saint-Martin R and Kreisel J 2008 arXiv:0712.0736v1

[16] Venkateswaran U D, Naik V M and Naik R 1998 *Phys. Rev.* B **58** 14256

[17] Janolin P E, Bouvier P, Kreisel J, Thomas P A, Kornev I A, Bellaiche L, Crichton W, Hanfland M and Dkhil B 2008 *Phys. Rev. Lett.* **101** 237201

[18] Kreisel J, Glazer A M, Bouvier P and Lucazeau G 2001 *Phys. Rev.* B **63** 174103

[19] Janolin P E, Dkhil B, Bouvier P, Kreisel J and Thomas P A 2006 *Phys. Rev.* B **73** 094128

[20] Chen J, Xing X R, Watson A, Wang W, Yu R B, Deng J X, Yan L, Sun C and Chen X B 2007 *Chem. Mater.* **19** 3598

[21] Gavriliuk A G, Struzhkin V V, Lyubutin I S, Hu M Y and Mao H K 2005 *JETP Lett.* **82** 224